Nexo Revista Científica
Vol. 34, No. 04, pp. 1490-1498/Septiembre 2021

ISSN-E 1995-9516
Universidad Nacional de Ingeniería

http://revistas.uni.edu.ni/index.php/Nexo
https://doi.org/10.5377/nexo.v34i04.12694

Performance dynamics of pdc cutters used in breaking ductile brittle rock

Dinámica del desempeño de los cortadores pdc durante la destrucción de las rocas frágiles y dúctiles

Oleg B. Trushkin*, Hamzja I. Akchurin

Ufa State Petroleum Technological University, Ufa, Russian Federation

*azimtrushkin@yandex.ru

(recibido/received: 26-mayo-2021; aceptado/accepted:05-agosto-2021)

ABSTRACT

The widespread application of cutting - chipping action bits with PDC cutters is held back due to the intense chipping and breakage of the latter. This article presents the results of bench-scale tests conducted to determine the values of three mutually perpendicular components of the load on sharp-edged and beveled rock-breaking cutters of 13.5 mm in diameter as well as the dynamic-response factors and mean square deviations (MSD) of these components. The forces change in time by leaps, which reflects the rock fracturing under the cutter. The MSD accepted as per-cycle amplitude is four times as low on average as the mean axial force; when a sharp-edged and a beveled cutter is used, the MSD is by 150 to 300 and by 300 to 500 % lower than the mean circumferential force.

Keywords: PDC bits; PDC cutters; Rock breaking; Three force components (axial, circumferential, and radial) of cutter load; Dynamic-response coefficients; Mean square deviation of forces.

RESUMEN

La aplicación generalizada de las brocas de acción de corte y astillado con fresas de PDC se ve frenada por el intenso astillado y la rotura de estas últimas. En este artículo se presentan los resultados de las pruebas a escala de banco realizadas para determinar los valores de tres componentes mutuamente perpendiculares de la carga en cortadores de roca de borde afilado y biselado de 13,5 mm de diámetro, así como los factores de respuesta dinámica y las desviaciones cuadráticas medias (MSD) de estos componentes. Las fuerzas cambian a saltos en el tiempo, lo que refleja la fractura de la roca bajo el cortador. La MSD aceptada como amplitud por ciclo es cuatro veces menor, por término medio, que la fuerza axial media; cuando se utiliza una fresa de bordes afilados y una biselada, la MSD es de un 150 a un 300 y de un 300 a un 500 % menor que la fuerza circunferencial media.

Palabras clave: Brocas PDC; Cortadores PDC; Destrucción de rocas; Tres componentes de la fuerza sobre el cortador (la axial, la circunferencial y la radial); Cocientes de respuesta dinámica; Desviación estándar de las fuerzas.

1. INTRODUCTION

The application of rock-breaking tools (RDT) with carbide-tipped diamond cutters and PDC bits and PDC core bits is largely limited by the intensive flaking and breakdowns of carbide-tipped diamond cutters, even of those with enhanced impact resistance (Besson et al., 2000; Borisov & Rubczov, 2014;

Kershenbaum, 2011; Nenashev et al., 2011; Neskoromnykh & Borisov, 2013). This is related to heavy impact loads on the cutters (Tretyak et al., 2019). One of the ways of upgrading the structure of RDT is to study the dynamics of the force parameters of their performance and assess the causes and determine the ways of minimizing the vibrations of these tools. There are several studies (Borisov, 2008; Borisov & Rubczov, 2014; Chulkova, 2012; Drilling Optimization, n.d.; Neskoromnykh & Borisov, 2013; Sharipov et al., 2013; Sharipov & Mingazov, 2012; Tretyak et al., 2019), where attempts have been made to analytically estimate the mean cutter load. However, the estimation proceeding from a large number of assumptions is very tentative. A more precise estimate is provided by the results of bench-scale tests conducted to reproduce the rock breaking process and perform correct measurements (Besson et al., 2000; Borisov, 2002, 2010; Glowka, 1987; Izbinski et al., 2015; Rafatian et al., 2010; Rajabov, 2012). However, these works pay almost no attention to the dynamic component of cutter loads. The source material for the article is the result of the testbed drilling of rock slabs using three PDC cutters (Trushkin, 2014, 2018; Trushkin & Akchurin, 2020).

2. MATERIALS AND METHODS

The test involved measuring the force load on PDC cutters used to break rock slabs with hardness by stamp p_{Mn}=950 mPa, yield strength p_0=650 mPa, and conventional ductility coefficient K = 1.7…2.

The cutters were 13.5 mm in diameter and had a sharp edge or a 0.3x45° bevel. A special test facility (Trushkin, 2014) was used to drill the rock slabs with three PDC cutters (Trushkin, 2018; Trushkin & Akchurin, 2020) which reproduced a drill bit profile, including the digital recording of three component loads on the central cutter. The directions of the recorded loads are shown in Fig. 1. Axial force F_g, circumferential force F_t, and radial force F_r were recorded at the sampling rate of 4 784 Hz of analogue signals from strain-gage sensors for each force parameter. The tests were conducted at three cutter position radii R=25, 50, and 85 mm, cutting head revolution frequency of 90 min^{-1}, and with the cutting zone rinsed with a water jet.

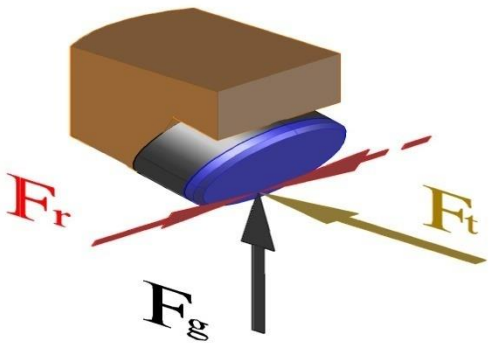

Figure 1. Recorded components of cutter load

3. RESULTS AND DISCUSSION

The cutting of subsurface rock is attended by its periodic fractures which result in significant changes in cutter load. A fragment of visualised changes in axial force F_g, circumferential force F_t, and radial force F_r observed at the time of using the beveled cutter with radius R=50 mm and footage per revolution δ=0.8 mm is shown in Fig. 2. It follows from Fig. 2 that the change in these forces over time is steplike, and their maxima and minima reflect the rock fracturing under the cutter. The broad limit of variation in the height of the maxima and depth of the minima on the diagrams is related to the influence of the rock's heterogeneity. The minima and maxima of the force relationships are synchronous, which confirms their relation to the specifics of subsurface rock disintegration.

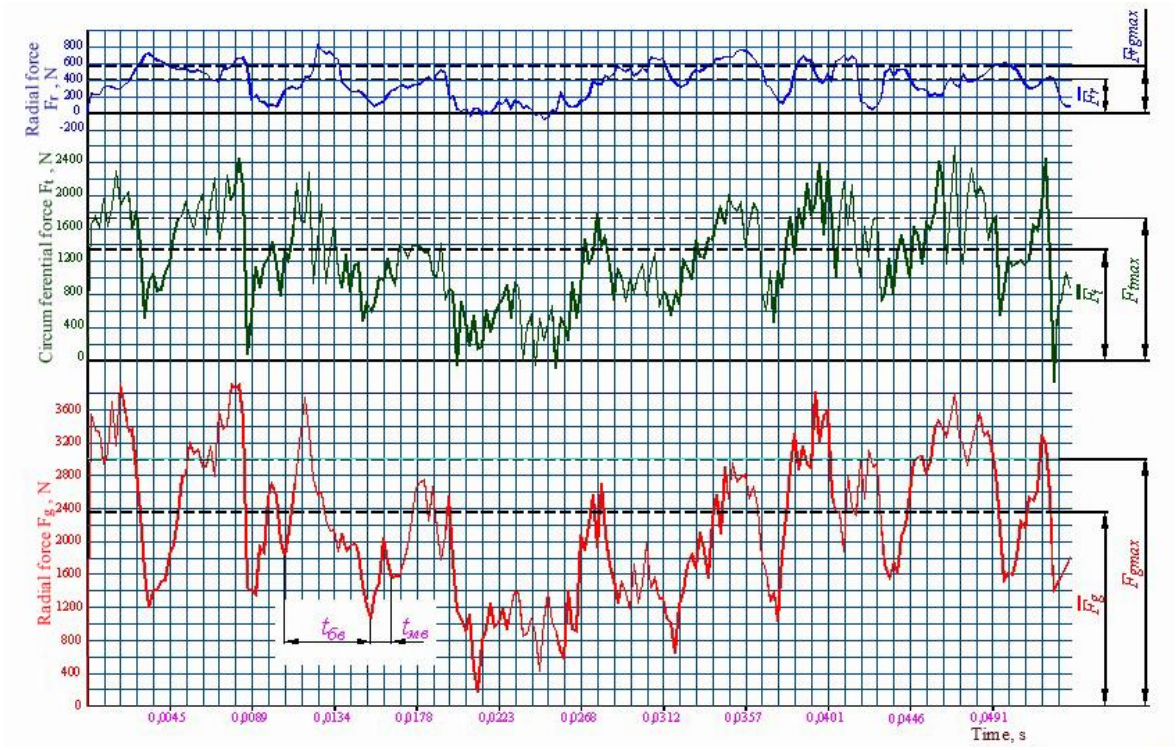

Figure2. Change of vertical (F_g), circumferential (F_t), and radial (F_r) loads on the beveled cutter over time

The plot of function $F_g=f(t)$ (Fig. 2) contains clearly distinguished oscillations which recur throughout half-period $t_{bind}$and are moduled at a high frequency with half-period t_{smind}. The load oscillations over time t_{bind} are related to big rock indents left under the cutter, whereas the load oscillations over time t_{smind} are related to more frequent smaller indents. The value of t_{bind} varies, which was why it was statistically estimated on the basis of 25 measurements conducted at each work radius of the cutter. The mean values of t_{bind} were used to calculate mean circumferential displacement Δl_t of the cutter and the number of big indents per revolution at footage per revolution δ=0.8 mm. It follows from the calculation results provided in Table 1 that the cutter's circumferential displacement corresponding to a big indent increases with an increase in the cutter's position radius R. Despite this fact, however, there is an increase in the number of big indents per one revolution of the drill bit.

It can be considered that the axial, circumferential, and radial force change over time in asymmetrical cycles of constant sign with several main parameters, such as mean value, amplitude, and frequency. It is well known that the cyclical loading of solid bodies results in their fatigue failure. The disintegration of the diamond layer and carbide substrate of PDC cutters are largely determined by their fatigue. The practice of using drill bits (Trushkin & Akchurin, 2020) shows that, the farther is the cutter from the drill bit centre, the higher is the probability of its breakdown. One of the reasons for this is a much higher number of loading cycles per revolution of the drill bit. To make the theoretical and experimental assessment of the influence of the cyclic loading of PDC cutters on their breakdown, it is necessary to know the mean value of the cycle and its amplitude and frequency.

The mean cycle value is determined by the mean force calculated in two phases: first of all, the mean force per revolution of the cutter head was calculated, and then the mean value of the 25 to 30 values calculated in the first phase was determined.

The quantity that should be taken for the cycle amplitude is the mean square deviation of a set of values (σ'_g,σ'_t, σ'_r), determined according to the mean force calculation procedure.

The frequency of loading cycles is determined by the number of big indents made per revolution. For the calculated frequency of loading cycles see Table 1.

Table 1. Circumferential cutter displacement corresponding to a big indent

Bottom radius*R*, mm	Mean circumferential cutter displacement Δl_t, mm	Mean square deviation Δl_t , mm	Drill bit turning angle corresponding to big indent, °	Number of big indents per drill bit revolution
25	0.56	0.08	1.28	281
50	0.65	0.09	0.74	486
85	0.78	0.07	0.53	679

The variation in load at rock breaking is usually characterized by a relative quantity represented by the dynamic-response coefficient. For example, the dynamic-response coefficient of the axial force is determined as

$$K_g = \mathrm{F}_{\mathrm{gmax}} / \bar{F}_g,$$

where $\bar{F}_g$ and F_{gmax} are the mean and the maximal axial force affecting the cutter, respectively.

The value of F_{gmax} at normal law of distribution F_g and 25 as the maximal number of observations is determined as

$$F_{g\max} = \bar{F}_g + \sigma'_g \cdot t_{1-p/2},$$

where σ'_g is the mean square deviation of the set of values of F_g and $t_{1-p/2}$ is the quantile of Student's t-distribution at a confidence coefficient of 1-p, where p is the significant level of 0.05 used in the calculations.

The dynamic-response coefficient of the circumferential (K_t) and radial (K_r) forces were determined in a similar manner.

The mean forces affecting the cutter at rock breaking depend on the footage per revolution. The graphs of the dependence of mean axial force $\overline{F}_g$, affecting the beveled cutter, on footage per revolution δ at three cutter's position radii *R* are presented in Fig. 3. The graphs contain confidence ranges calculated with a probability of 0.95. It follows from the graphs that the mean axial force in the examined range of footage per revolution varies from 700 to 2 800 N. The graph also contains two distinct axial force variation regions which indicate the steplike kind of rock breaking at cutting. In failure region I the cutter load intensively rises with a rise in the footage per revolution. However, the load sharply decreases with the expansion of the second region (II).

As shown by analyzing the similar graphs drawn for the sharp-edged cutter, the mean axial force varies from 300 to 1 400 N; that said, the influence of radius *R*is ambiguous. The minimal and the maximal values of $\overline{F}_g$ are observed at *R*=25 and 50 mm, respectively. The axial force variation pattern also reflects the steplike kind of rock breaking at cutting. Three characteristic regions are distinguished. In failure region I the cutter load intensively rises with a rise in the footage per revolution. As region II expands, the load sharply decreases and then begins to rise. As region III begins to expand, the load stabilizes with a minor decrease. As shown by comparing the axial force variation ranges of the sharp-edged and the beveled cutter, the mean axial force required to achieve equal footage per revolution for the beveled cutter is by 80 to 130 % higher than for the sharp-edged cutter.

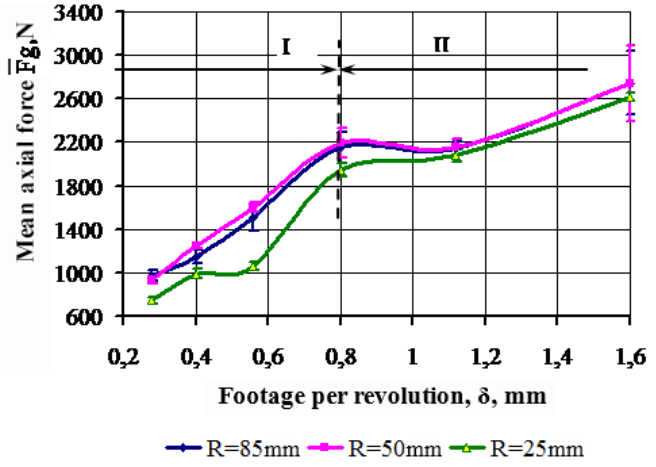

Figure 3. Dependence of mean axial force $\overline{F_g}$ on footage per revolution δ, affecting the beveled cutter

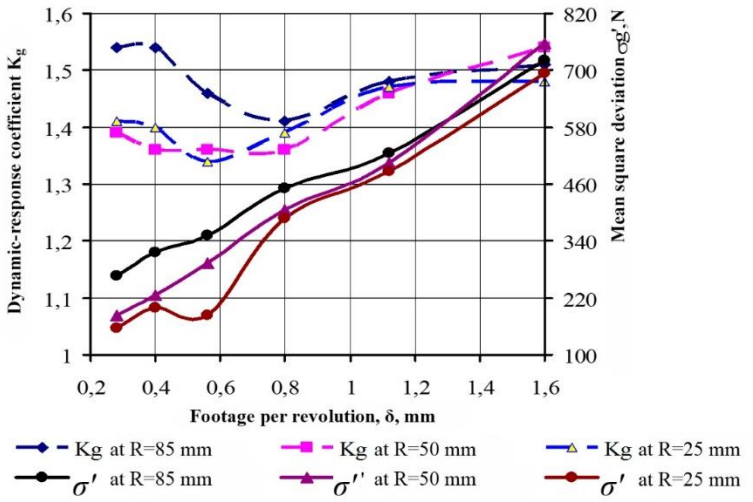

Figure 4. Dependences of dynamic-response coefficients *Kg* and MSD *σ'g* of axial force *Fg* for the beveled cutter

The graphs of relationships $K_g = f(\delta)$ and $\sigma'_g = q(\delta)$ for the beveled cutter are shown in Fig. 4. According to these graphs, K_g varies from 1.3 to 1.6. Mean square deviation σ'_g taken for the cycle amplitude steadily rises with an increase in the footage per revolution and is four times as small on average as the mean force but for the interval at *R*=50 mm.

As shown by analyzing the similar diagrams for the sharp-edged cutter, in the first failure region selected in the graph of $\overline{F_g} = f(\delta)$ σ'_g intensively rises, whereas in the second and third region this intensity decreases; that said, the MSD is four times as small on average as the mean axial force. It should be noted that there is a certain regularity observed: σ'_g rises with an increase in *R*. The variation range of K_g does not differ much from the range for the beveled cutter.

It is interesting to analyze mean circumferential force $\overline{F_t}$ as the component of the rock-breaking tool torque. The diagrams of the $\overline{F_t}=f(\delta)$ function for the beveled cutter at three radii *R* with marked confidence ranges calculated with a probability of 0.95 are shown in Fig. 5. The kind of the $\overline{F_t}=f(\delta)$function is fully identical to the kind of the $\overline{F_g}=f(\delta)$ function, which includes the selection of two characteristic rock failure regions (see Fig. 3). Circumferential force $\overline{F_t}$ varies from 500 to 1 600

N. As shown by comparing the variation ranges of the axial and the radial force, the axial force is by 60 % greater on average than circumferential.

As shown by analyzing the similar diagrams for the sharp-edged cutter, circumferential force $\overline{F_t}$ varies from 300 to 1 400 N and there are three characteristics rock failure regions distinguished depending on the footage per revolution. As shown by comparing the variation ranges of the axial and the circumferential force, these ranges are almost equal for the sharp-edged cutter. As shown by comparing the variation ranges of circumferential forces, the average circumferential force required for producing an equal rock-breaking effect when using the beveled cutter is by 10 to 60 % greater than the one produced using the sharp-edged cutter. Therefore, the PDC drill bits with the sharp-edged cutter can be expected to deliver a higher torque (Trushkin et al., 2016).

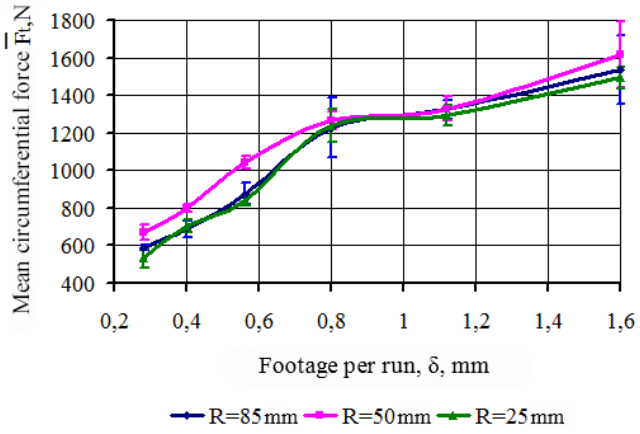

Figure 5. Dependence of mean circumferential force $\overline{F_t}$ on footage per revolution δ, affecting the beveled cutter

The graphs of the dependence of dynamic-response coefficients K_t and MSD σ'_t of circumferential force$\overline{F_t}$ on footage per revolution δ for the beveled cutters are presented in Fig. 6.

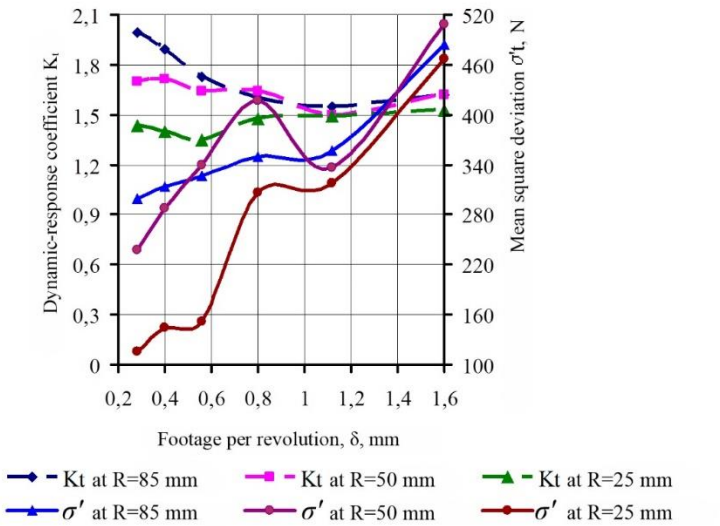

Figure 6. Dependences of dynamic-response coefficients *Kt* and MSD *σ't of* circumferential force $\overline{F_t}$for the beveled cutter

The dynamic-response coefficients vary from 1.35 to 1.75. The variation pattern of K_t reflects the steplike kind of rock breaking. Mean square deviation σ'_t rises intermittently from 100 to 500 N with an increase in δ and is four to six times as small as the circumferential force. When the sharp-edged

cutter is used, σ'_t rises almost monotonously within the same limits and is by 150 to 300 % smaller than the mean circumferential force.

Radial force $\overline{Fr}$ is one of the causes of the transverse displacements of the rock-breaking tool.

The diagrams of the relationship of the radial force to the footage per revolution for the beveled cutter and additional ranges calculated with a probability of 0.95 are shown in Fig. 7.

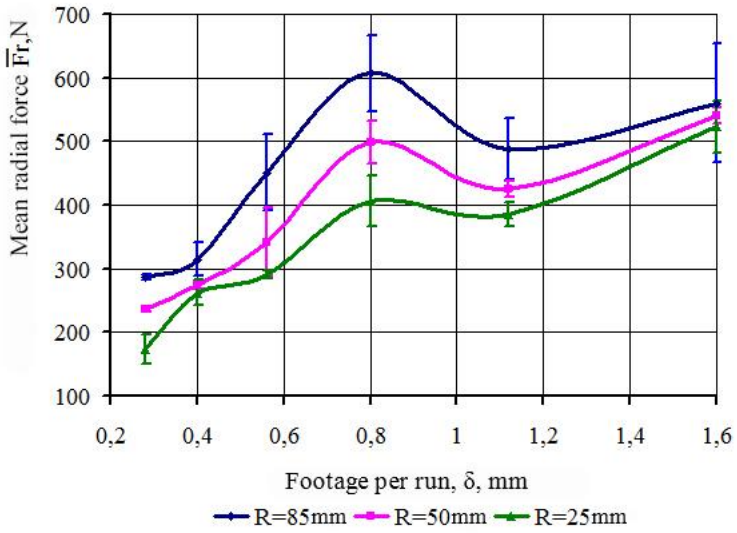

Figure 7. Dependence of mean radial force F_r on footage per revolution δ, affecting the beveled cutter

As seen from these diagrams, when the beveled cutter is used, the mean radial force intensively rises in the first region and stabilizes in the second, and ranges from 160 to 600 N. When comparing the changes in mean circumferential force $\overline{Ft}$ and radial force $\overline{Fr}$, it should be noted that, in the analyzed cutter layout pattern, the mean radial load is by 170 to 210 % smaller.

The dynamic-response coefficient of the radial force ranges from 1.43 to 1.9 and is much higher than the dynamic-response coefficients of the axial and the radial force.

The radial force of using the sharp-edged cutter ranges from 75 to 260 N, which is by 100 to 130 % smaller than the load on the beveled cutter, whereas the dynamic-response coefficient ranges from 1.55 to 3.15.

The results of experimentally investigating the level and kind of changes in the component loads on PDC cutters and also their dynamic-response coefficients and MSD at the failure of medium-hard ductile brittle rock can be used in updating and developing cutter endurance test methods and the procedure of cutter longevity examination tests at different drill bit radii (Trushkin & Akchurin, 2020).

4. CONCLUSION

The use of PDC cutters for rock breaking is attended by steplike changes in axial, circumferential, and radial forces over time, and the maximal and minimal values of these forces point to the rock fracturing under the cutter. The minima and maxima of the dependences of the axial, circumferential, and radial forces coincide in time, which confirms their relation to the specifics of rock breaking. The pattern of change in the mean axial and circumferential force, depending on the footage per revolution in the analyzed value range, allows distinguishing three and two distinct rock breaking regions when using the sharp-edged and the beveled cutter, respectively. The axial and the mean circumferential

force required to achieve equal footage per revolution in case of using the beveled cutter are by 80 to 130 and by 10 to 60 % greater than for the sharp-edged cutter, which means that a larger torque must be expected from PDC drill bits with sharp-edged cutters.

In the examined cutter layout the mean radial force of using the sharp-edged and the beveled cutter is by 300 to 440 and, respectively, by 170 to 210 % weaker than the circumferential cutting force.

It is proposed to estimate variations in cutter loads not only using the conventional dimensionless dynamic-response coefficient but also the dimensional quantity represented by the mean square deviation.

In case of using the sharp-edged and the beveled cutter, the dynamic-response coefficients of the axial and circumferential force range from 1.35 to 1.75. The range of variations in the dynamic-response coefficient of the radial forces is 1.43 to 1.9 for the beveled cutter and 1.55 to 3.15 for the sharp-edged cutter. The variation pattern of the dynamic-response coefficients reflects the steplike pattern of rock disintegration.

It can be reckoned that the changes in the axial, circumferential, and radial force over time occur in asymmetrical cycles of constant sign, with the main parameters including the mean value, amplitude, and frequency. It is well known that the cyclical loading of solid bodies results in their fatigue failure. The disintegration of the diamond layer and carbide substrate of PDC cutters can be largely determined by their fatigue.

The results of the operational tests of PDC cutters can be used in calculating the force performance parameters of respective drill bits and to develop facilities and procedures for exposing cutters to impact load and endurance tests.

REFERENCIAS

Besson, A., Berr, B., Dillard, S., Drake, E., Ivie, B., Ivie, C., Smith, R., & Watson, G. (2000). On the Cutting Edge. *Oilfield Review, 12*(3), 36–57.

Borisov, K. I. (2002). Experimental Numerical Evaluation of Power Characteristics of Rock Cutting. *Bulletin of the Tomsk Polytechnic University, 305* (8), 216–219.

Borisov, K. I. (2008). Procedure of Evaluating the Efficiency of Dynamic Rock Fracture by Cutting-Shearing Tools. *Oil Industry, 8*, 46–47.

Borisov, K. I. (2010). Performance Dynamics of Cutters Used in Rock Breaking by Cutting-Shearing PDC Tools. *Bulletin of the Tomsk Polytechnic University, 317*(1), 161–164.

Borisov, K. I., & Rubczov, V. L. (2014). Analytical Study of Temporal Strength Characteristic of Rock at its Braking and Cutting by Means of PDC Cutters. *Bulletin of the Tomsk Polytechnic University, 2014*(1), 172–178.

Chulkova, V. V. (2012). Experience in Using PDC Bits in Interstratified Solid Beds in the Volga-Ural Region. *Bulletin of the Association of Drilling Contractors, 2*, 58–61.

Drilling Optimization. http://www.bakerhughes.com/products-and-services/drilling/drill-bit-systems/drilling-optimization/innovation-and-technology

Glowka, D. A. (1987). *Development of a Method for Predicting the Performance and Wear of PDC Drill Bits.* Sandia Report No. SAND86-1745. Albuquerque, New Mexico: Sandia National Laboratories.

Izbinski, K., Patel, S. G., & van Deven, A. (2015). *Baker Hughes Incorporated. Innovative Dual-Chamfer Edge Technology Leads to Performance Gains in PDC Bits.* London: SPE/IADC Drilling Conference and Exhibition. Paper SPE-173157-MS.

Kershenbaum, V. Ya. (Ed.) (2011). Rock-Breaking Drill Tools. Drill Bits with Fixed Diamond-Bearing Cutters. *International Reference Guide. Vol. 2*. Moscow: National Institute of Oil and Gas "Gubkin University".

Nenashev, M. V., Ibatullin, I. D., Zhuravlev, A. N., & Kosulin, S. I. (2011). Technical Means and Procedures of Receipt Quality Examination of PDC Teeth of Diamond Drill Bits. *Izvestia of the Samara Scientific Centre of the Russian Academy of Sciences, 13* (4/3), 835–838.

Neskoromnykh, V. V., & Borisov, K. I. (2013). Analytical Study of Rock Cutting and Shearing by Drill Bit with PDC cutters. *Bulletin of the Tomsk Polytechnic University, 323* (1), 191–195.

Rafatian, N., Miska, S., Ledgerwood, L. W. W., Ahmed, R., Yu, M., & Takach, N. (2010). *Experimental Study of MSE of a Single PDC Cutter Interacting with Rock under Simulated Pressurized Conditions*. SPE Drilling & Completion, 25(1), 10–18. Paper SPE-119302-PA.

Rajabov, V., Yu, M., Miska, S., Takach, N., Mortimer, L., & Ozbayoglu, Evr. (2012). *The Effects of Back Rake and Side Rake Angles on Mechanical Specific Energy of Single PDC Cutters with Selected Rocks at Varying Depth of Cuts and Confining Pressures*. San Diego, California: IADC/SPE Drilling Conference and Exhibition. Paper SPE 151406-MS.

Sharipov, A. N., Khramov, D. G., & Kovalevskiy, E. A. (2013). Optimizing PDC Bit Design to Reduce Production Section Drilling Time. *Drilling and Oil, 6*, 46–50.

Sharipov, A. N., & Mingazov, R. R. (2012). Solid Rock Drilling Bits. *Drilling and Oil, 12*, 46–50.

Tretyak, A. Ya., Kuznetsova, A. V., & Borisov, K. A. (2019). Determining PDC Cutter Breakdowns by Regression and Neural Network Modeling. *Bulletin of the Tomsk Polytechnic University, 330* (5), 169–177.

Trushkin, O. B. (2014). Bench for Power and Energy Load Tests of PDC Bit Cutters. In: *Proceedings of the Third All-Russian Research and Engineering Conference "Innovative Oil and Gas Equipment: Problems and Solutions",* pp. 13–16. Ufa: Ufa Petroleum State Technological University.

Trushkin, O. B. (2018). Measuring PDC Cutter Load during Testbed Drilling. *Automation, Telemetry, and Communication in Petroleum Industry, 3*, 5–10.

Trushkin, O. B., & Akchurin, H. I. (2020). PDC Cutter Pressure on Plastic-Brittle Rock in the Process of its Destruction. *Journal of Mining Institute, 244*, 448–453.

Trushkin, O. B., Popov, A. N., & Trushkin, B. N. (2016). Particularities of Torque and Energy Consumption by Bits, Equipped by Cutters with Chamfer on the Cutting Edge. *Oil and Gas Territory, 12*, 26–29.

SEMBLANCE OF THE AUTHORS

Oleg B. Trushkin: He is a Candidate of Engineering Sciences, Associate Professor at the Department of Oil and Gas Well Drilling of "Ufa State Petroleum Technological University" (USPTU). His fields of scientific interests include study of the operation of rock cutting and drilling tools (including in the process of drilling) in order to improve their designs and operating modes.

Hamzja Ish. Akchurin: He is a Candidate of Engineering Sciences, Senior Research Officer, Professor at the Department of Oil and Gas Well Drilling of "Ufa State Petroleum Technological University" (USPTU). His fields of scientific interests include study of the operation of rock cutting and drilling tools (including in the process of drilling) in order to improve their designs and operating modes.